

# MASQuant: Modality-Aware Smoothing Quantization for Multimodal Large Language Models

Lulu Hu\*    Wenhui Xiao\*    Xin Chen\*    Xinhua Xu    Bowen Xu<sup>†</sup>    Kun Li  
 Yongliang Tao

Alibaba Cloud Computing, Alibaba Group

{chudu.hll, wenhu.xwh, andy.cx, bowen.xbw}@alibaba-inc.com

## Abstract

*Post-training quantization (PTQ) with computational invariance for Large Language Models (LLMs) have demonstrated remarkable advances, however, their application to Multimodal Large Language Models (MLLMs) presents substantial challenges. In this paper, we analyze SmoothQuant as a case study and identify two critical issues: Smoothing Misalignment and Cross-Modal Computational Invariance. To address these issues, we propose Modality-Aware Smoothing Quantization (MASQuant), a novel framework that introduces (1) Modality-Aware Smoothing (MAS), which learns separate, modality-specific smoothing factors to prevent Smoothing Misalignment, and (2) Cross-Modal Compensation (CMC), which addresses Cross-modal Computational Invariance by using SVD whitening to transform multi-modal activation differences into low-rank forms, enabling unified quantization across modalities. MASQuant demonstrates stable quantization performance across both dual-modal and tri-modal MLLMs. Experimental results show that MASQuant is competitive among the state-of-the-art PTQ algorithms. Source code: <https://github.com/alibaba/EfficientAI>.*

## 1. Introduction

Post-training quantization (PTQ) has become essential for deploying Large Language Models (LLMs) [1, 9, 32] on resource-constrained devices, and this need is amplified for Multimodal Large Language Models (MLLMs), which demonstrate impressive cross-modal reasoning capabilities [11, 13, 17, 29, 42, 43]. PTQ methods based on computational invariance [19, 24, 27, 31, 36, 37], particularly channel-wise smoothing [19, 27, 37], have proven highly effective for text-only LLMs by redistributing activa-

tion outliers through channel-level scaling factors. Recent work has also begun recognizing MLLM-specific characteristics—MBQ [16] observes unequal contributions of visual and text tokens to quantization error, while MQuant [41] finds that visual token activations exhibit much higher magnitudes than text tokens. However, the direct application of channel-wise smoothing to MLLMs remains surprisingly underexplored, raising an important question: do these successful channel-wise smoothing PTQ methods transfer seamlessly to the multimodal setting?

Through systematic analysis of vision-language and omni-modal MLLMs [3, 39], we identify a fundamental problem. Different modalities exhibit vastly different activation magnitudes—visual tokens typically show ranges 10–100× larger than text and audio tokens. Channel-wise smoothing computes a single scaling factor per channel, but when modalities with such disparate distributions pass through the same layer, the dominant modality’s larger activations dictate the smoothing factor. Activations from non-dominant modalities thus become over-smoothed, crushing their signal and causing severe quantization errors. We term this phenomenon smoothing misalignment. A natural solution is to compute separate smoothing factors for each modality. However, this seemingly simple solution introduces a critical flaw: preserving computational invariance under this scheme requires storing distinct quantized weights for each modality. This defeats the fundamental purpose of quantization, which aims to reduce memory footprint through a single low-precision weight representation. The question becomes: *can we collect modality-specific smoothing factors while maintaining a single quantized weight for inference?*

We address this challenge through Modality-Aware Smoothing Quantization (MASQuant). Our key idea is to learn dedicated smoothing factors for each modality, but during inference, we use the text-smoothed weights as a base and apply modality-specific low-rank compensation. This design simultaneously resolves smoothing misalignment and preserves computational invariance. Specifically,

\*Equal contribution.

<sup>†</sup>Corresponding author

Modality-Aware Smoothing (MAS) optimizes smoothing factors directly for each modality’s activations, eliminating smoothing misalignment and pushing channel-wise smoothing to its optimization limit. To maintain a single weight representation, Cross-Modal Compensation (CMC) leverages a key observation: differences in smoothed activations across modalities are low-rank. We prove this mathematically and use SVD-based whitening to transform these differences into compact low-rank matrices. By compensating for modality-induced variations through lightweight low-rank corrections to the text-smoothed base weights, MASQuant achieves modality-specific adaptation without sacrificing the unified weight structure essential for efficient quantization.

We evaluate MASQuant across diverse MLLM architectures spanning vision-language and omni-modal configurations. Results across all evaluated benchmarks demonstrate consistent superiority over existing channel-wise smoothing PTQ methods.

In summary, our main contributions are:

- We identify and formalize smoothing misalignment—the fundamental obstacle in applying channel-wise smoothing PTQ to MLLMs—and resolve it through Modality-Aware Smoothing.
- We prove that inter-modal activation differences are low-rank, enabling Cross-Modal Compensation to maintain computational invariance with a single set of quantized weights.
- We present MASQuant, a PTQ method that is effective on both vision-language and omni-modal MLLMs.

## 2. Related Work

**LLMs Quantization.** LLM quantization methods are broadly categorized into *Quantization-Aware Training* (QAT) [4, 6, 21] and *Post-Training Quantization* (PTQ) [19, 27, 37]. QAT incorporates quantization into training to adapt models to low-precision computation, while PTQ applies quantization directly using calibration data. PTQ approaches include: (1) error compensation via second-order gradients [10] or low-rank correction [40, 44]; (2) channel-wise smoothing to mitigate outliers [19, 24, 27, 31, 37]; (3) rotation-based distribution restructuring [2, 5, 22]; and (4) mixed-precision strategies [7, 14, 45].

**MLLMs Quantization.** Quantizing MLLMs presents unique challenges due to cross-modal activation disparities. MQuant [41] identifies that visual token activations can exceed textual ones by 20×, proposing modality-specific quantization. MBQ [16] observes visual tokens are less quantization-sensitive and introduces gradient-weighted error balancing. QSLAW [38] addresses increased outlier density from multimodal inputs through learnable weight-group scaling. Despite these advances, activation quan-

tization remains inadequately addressed, motivating our modality-aware smooth quantization approach.

## 3. Preliminaries

### 3.1. Computational Invariance based PTQ

PTQ addresses significant computational and storage challenges by mapping high-precision floating-point tensor  $\mathbf{x}$  to low-precision  $N$ -bit integer tensor  $\hat{\mathbf{x}}_N$ :

$$\hat{\mathbf{x}}_N = Q(\mathbf{x}) = \left( \text{clamp} \left( \left\lfloor \frac{\mathbf{x}}{\Delta} \right\rfloor + z, q_{\min}, q_{\max} \right) - z \right) \cdot \Delta, \quad (1)$$

where  $\Delta$  is the scale factor,  $z$  is zero-point,  $\lfloor \cdot \rfloor$  is the rounding-to-nearest operator, and  $\text{clamp}$  clips values outside the integer range  $[q_{\min}, q_{\max}]$ . We use  $WxAy$  notation for  $x$ -bit weights and  $y$ -bit activations, with two main types: weight-only quantization (e.g., W4A16) and weight-activation quantization (e.g., W8A8, W4A8). For a linear layer  $\mathbf{Y} = \mathbf{XW}$ , where  $\mathbf{X} \in \mathbb{R}^{T \times D_{\text{in}}}$ ,  $\mathbf{W} \in \mathbb{R}^{D_{\text{in}} \times D_{\text{out}}}$ , the layer can be reformulated based on computational invariance as:

$$\mathbf{Y} = (\mathbf{XS}^{-1}) \cdot (\mathbf{SW}), \quad (2)$$

where  $\mathbf{S}$  can be diagonal matrix [19, 27, 37] or orthogonal matrix [5, 18, 22, 31].  $\mathbf{S}$  reduces the outliers in  $\mathbf{X}$  and lead to better quantization reconstruction loss:

$$L = \mathcal{L}(Q(\mathbf{XS}^{-1}) \cdot Q(\mathbf{SW}), \mathbf{XW}). \quad (3)$$

In this paper, we demonstrate that applying  $\mathbf{S}$  for different modalities in MLLMs can achieve robust and effective PTQ performance.

### 3.2. SVD-based Whitening

Prior work [34, 35] uses SVD-based whitening for low-rank weight compression. Given input activations  $\mathbf{X}$  and weights  $\mathbf{W}$ , the whitening transform is derived by decomposing the activation covariance:

$$\mathbf{P}\mathbf{\Lambda}\mathbf{P}^\top = \text{SVD}(\mathbf{X}^\top\mathbf{X}). \quad (4)$$

A whitening matrix  $\mathbf{T} = (\mathbf{P}\mathbf{\Lambda}^{1/2})^\top$  transforms  $\mathbf{XW}$  into  $(\mathbf{XT})(\mathbf{T}^{-1}\mathbf{W})$  which satisfies  $(\mathbf{XT}^{-1})^\top(\mathbf{XT}^{-1}) = \mathbf{I}$ , yielding whitened activations. SVD-LLM v2 [35] shows that performing SVD on  $\mathbf{TW}$  and truncating to rank  $r$  minimizes reconstruction error  $\|\mathbf{XW} - \mathbf{XW}'\|_F$ :

$$\mathbf{U}, \mathbf{S}, \mathbf{V} = \text{SVD}(\mathbf{TW}), \quad (5)$$

$$\mathbf{U}_r, \mathbf{S}_r, \mathbf{V}_r = \text{Trunc}_r(\mathbf{U}, \mathbf{S}, \mathbf{V}), \quad (6)$$

$$\mathbf{W}' = \mathbf{T}^{-1}\mathbf{U}_r\mathbf{S}_r\mathbf{V}_r. \quad (7)$$

While existing methods apply whitening for weight compression, we are the first to show that whitening can effectively compensate for cross-modal weight differences, enabling unified quantization across modalities.

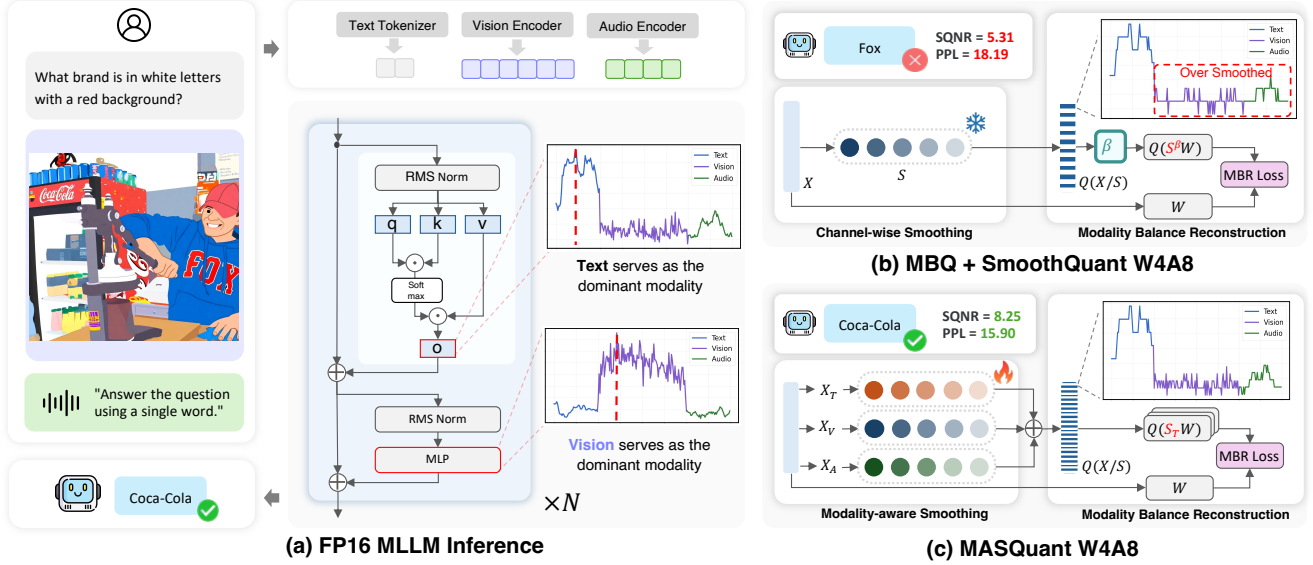


Figure 1. (a). Activation distributions during multimodal reasoning in MLLMs. Different dominant modalities emerge across MLLM components, leading to failure of general PTQ methods that diminish vision importance. (b). Impact of SmoothQuant’s uniform smoothing factors  $S$  computation on MLLM quantization performance (low SQNR, high PPL). (c). MASQuant addresses smoothing misalignment through the combination of MAS and CMC, thereby significantly enhancing PTQ performance in MLLMs. MBR Loss indicates Modality Balanced Reconstruction Loss.

## 4. MASQuant

In this section, we present our Modality-Aware Smooth Quantization (MASQuant) framework includes Modality-Aware Smoothing (MAS) followed by Cross-Modal Compensation (CMC), designed to address the critical issue of smoothing misalignment and cross-modal computational invariance in MLLMs.

### 4.1. Motivation

**Revisiting Smoothing Factors.** Existing methods compute smoothing factors  $s$  through closed-form solutions. SmoothQuant [37] uses:

$$s_i = \frac{\max_t |x_{t,i}|^\beta}{\max_j |w_{j,i}|^{1-\beta}}, \quad (8)$$

while AWQ [19] adopts:

$$s_i = \left( \frac{\sum_{t=1}^n |x_{t,i}|}{n} \right)^\beta, \beta^* = \arg \min_{\beta} L(s). \quad (9)$$

MBQ [16] extends this to MLLMs by adjusting the contribution of different modality activations when searching for  $\beta$  values. However, all these methods optimize only the hyperparameter  $\beta$  while the smoothing factors themselves are never treated as free parameters. OmniQuant [27] demonstrates that learnable smoothing factors can better minimize quantization error, we adopt this principle for MLLMs—instead of searching over  $\beta$ , we directly optimize matrix  $S$

whose diagonal entries are smoothing factors  $s_i$ :

$$S^* = \arg \min_S \mathcal{L}(Q(XS^{-1})Q(SW), XW). \quad (10)$$

This formulation is more flexible—it can discover optimal smoothing patterns beyond what any  $\beta$ -parameterized formula can express.

**Smoothing Misalignment.** MLLMs process multiple modalities with vastly different activation magnitudes [41]. we measure the activation range per channel:  $\mathbf{R}_i^m = \max_t |x_{t,i}^m|$  for modality  $m \in \mathcal{M}$ , where  $x_{t,i}^m$  is the activation of the  $t$ -th token in channel  $i$ . When calibrating on mixed-modality data, the unified smoothing factor is determined by the maximum range across all tokens:

$$s_i^{\text{uni}} = \frac{(\max_t |x_{t,i}|)^\beta}{(\max_j |w_{j,i}|)^{1-\beta}} = \frac{(\max_{m,t} |x_{t,i}^m|)^\beta}{(\max_j |w_{j,i}|)^{1-\beta}} \propto \mathbf{R}_i^{m^*}, \quad (11)$$

where  $m^* = \arg \max_m \mathbf{R}_i^m$  is the dominant modality. This unified factor  $s_i^{\text{uni}}$  aligns with the dominant modality’s ideal factor but severely mismatches others—a phenomenon we term smoothing misalignment. Non-dominant modalities suffer degraded quantization quality as their activations are scaled by factors optimized for a different magnitude regime. Figure 1 illustrates this phenomenon in detail.

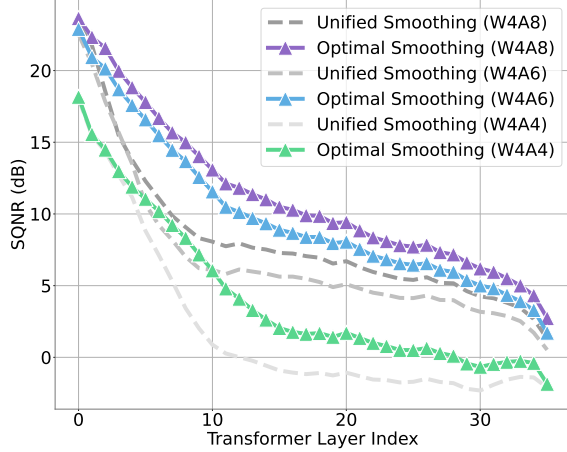


Figure 2. Comparative analysis of SQNR degradation of Qwen2.5-Omni-3B under multimodal input condition. We selected 32 samples from OmniBench and computed the average SQNR for each layer.

## 4.2. Modality-Aware Smoothing

Smoothing misalignment arises from unified scaling across heterogeneous modalities. We address this by maintaining modality-specific smoothing factors, eliminating dominance at its root. Let  $\mathcal{M}$  denote the set of supported modalities (e.g., text, image, audio). For each modality  $m \in \mathcal{M}$ , we first obtain the initial values of the modality-aware smoothing factors  $\mathbf{S}_m \in \mathbb{R}^{d \times d}$ :

$$\mathbf{S}_m = \text{diag}(\mathbf{s}^m), \quad s_i^m = \sqrt{\frac{\max_t |x_{t,i}^m|}{\max_j |w_{j,i}|}}, \quad m \in \mathcal{M}. \quad (12)$$

We then optimize the  $\mathbf{S}_m$  by minimizing MAE loss [16] on modality-specific data, We simplify the notation  $\{\mathbf{S}_m\}_{m \in \mathcal{M}}$  as  $\{\mathbf{S}_m\}$  for brevity:

$$\{\mathbf{S}_m^*\} = \arg \min_{\{\mathbf{S}_m\}} \sum_{m \in \mathcal{M}} (\lambda_m \cdot \mathcal{L}_{\text{MAE}}(\mathbf{S}_m, \mathbf{X}_m, \mathbf{W})), \quad (13)$$

where  $\lambda_m$  denotes the loss weight for modality  $m$ . For modality  $m$ , the quantization reconstruct MAE loss is:

$$\mathcal{L}_{\text{MAE}} = \|\mathbf{Q}(\mathbf{X}_m \mathbf{S}_m^{-1}) \cdot \mathbf{Q}(\mathbf{S}_m \mathbf{W}) - \mathbf{X}_m \mathbf{W}\|. \quad (14)$$

This ensures  $\mathbf{S}_m^*$  captures modality-specific statistics without cross-modality interference. We quantify benefit of  $\mathbf{S}_m$  through SQNR [28, 33] analysis. For a token  $\mathbf{x}_t$ , SQNR measures quantization quality as:

$$\text{SQNR}(\mathbf{x}_t) = 10 \log_{10} \left( \frac{\|\mathbf{x}_t\|^2}{\|\mathbf{x}_t - \mathbf{Q}(\mathbf{x}_t)\|^2} \right), \quad (15)$$

Under channel-wise smoothing with smoothing factor  $s$ , when  $\mathbf{x}_t \gg \Delta_t$  in Equation 1, quantization error  $e_t$  can

be approximated as uniformly distributed over  $[-\frac{\Delta_t}{2}, \frac{\Delta_t}{2}]$ . Thus, the mean squared error across  $d$  channels is  $d \cdot \frac{\Delta_t^2}{12}$ . This yields SQNR of SmoothQuant (omitting constants):

$$\text{SQNR}(\mathbf{s}, \mathbf{x}_t) \propto \frac{\sum_{i=1}^d \left\| \frac{x_{t,i}}{s_i} \right\|^2}{d \cdot \frac{\Delta_t^2}{12}} \propto \frac{\sum_{i=1}^d \left( \frac{x_{t,i}}{s_i} \right)^2}{\left( \max_i \left| \frac{x_{t,i}}{s_i} \right| \right)^2}, \quad (16)$$

based on which the degradation can be quantified.

**Theorem 1.** [SQNR Degradation under Smoothing Misalignment] Consider a layer processing multimodal inputs with dominant modality  $m$  and non-dominant modality  $m'$ . Let  $\alpha_i^{m,m'} = R_i^m / R_i^{m'}$  denote the range ratio at channel  $i$ , where  $R_i^m$  and  $R_i^{m'}$  are the activation ranges. Using unified smoothing  $\mathbf{s}^{\text{uni}} \approx \mathbf{s}^m$  yields SQNR degradation (exact as  $\alpha^{m,m'} \gg 1$ ):

$$\begin{aligned} \text{SQNR}(\mathbf{s}^{\text{uni}}, \mathbf{x}_t^{m'}) &= \text{SQNR}(\mathbf{s}^{m'}, \mathbf{x}_t^{m'}) \\ &\quad - 10 \log_{10} \left( \frac{d(\min_i (\alpha_i^{m,m'})^2)}{\sum_{i=1}^d \frac{1}{(\alpha_i^{m,m'})^2}} \right). \end{aligned} \quad (17)$$

*Proof.* To simplify notation, we let  $x_i = x_{t,i}^{m'}$ ,  $R = R_i^{m'}$ , and  $\alpha_i = \alpha_i^{m,m'}$ . We compare the upper bounds of the SQNR for the token  $\mathbf{x}_t^{m'}$  under two smoothing strategies, which are achieved when the token’s activations are uniform across channels (i.e.,  $x_1/R_1 \approx x_2/R_2 \approx \dots \approx x_d/R_d$ ): The SQNR for optimal smoothing is proportional to the dimension  $d$ :

$$\text{SQNR}(\mathbf{s}^{m'}, \mathbf{x}) = 10 \log_{10} \frac{\sum_{i=1}^d (x_i/R_i)^2}{(\max_i |x_i/R_i|)^2} = 10 \log_{10} d, \quad (18)$$

and SQNR for unified smoothing upper bound is given by:

$$\text{SQNR}(\mathbf{s}^{\text{uni}}, \mathbf{x}) = \log_{10} \frac{\sum_{i=1}^d 1/\alpha_i^2}{(\max_i 1/\alpha_i)^2}. \quad (19)$$

The difference between the two SQNR upper bounds is:

$$\Delta = 10 \log_{10} \underbrace{\left( \frac{1}{d \cdot (\max_i \frac{1}{\alpha_i})^2} \sum_{i=1}^d \frac{1}{\alpha_i^2} \right)}_{\leq 0, \text{ equality iff } \alpha_1 = \dots = \alpha_d}. \quad (20)$$

□

The results in Figure 2 validate Theorem 1 and Figure 4c and 4d provide distribution of  $\alpha_i^{m,m'}$  is non-uniform. Based on this, the inference process of the MAS becomes as follows:

$$\mathbf{Y} = \mathbf{Q}(\mathbf{X}_m \mathbf{S}_m^{-1}) \cdot \mathbf{Q}(\mathbf{S}_m \mathbf{W}), \quad m \in \mathcal{M}. \quad (21)$$

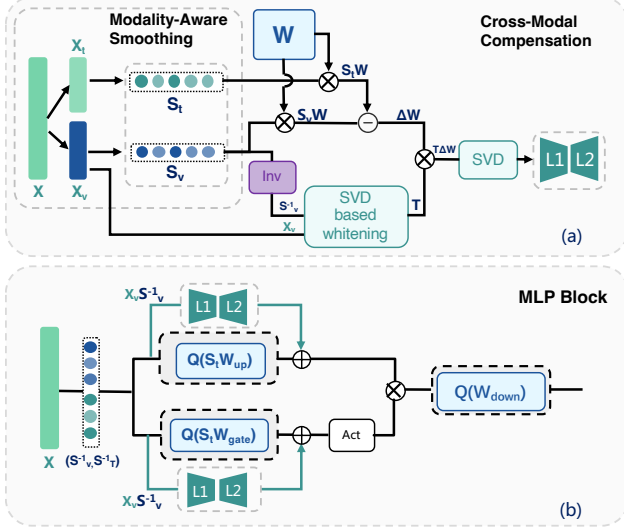


Figure 3. The illustrated case demonstrates a text-vision dual-modal setting. (a) Schematic workflow of MAS and CMC with calibration data, (b) Illustration of how low-rank matrices  $L_1$  and  $L_2$  in CMC are utilized in MASQuant, exemplified with an MLP block.

### 4.3. Cross-Modal Compensation

While MAS eliminates smoothing misalignment, it produces modality-specific quantized weight matrices  $Q(S_m W)$  that violate computational invariance—PTQ requires a single quantized weight across all modalities.

Our strategy is to store only one quantized weight  $Q(S_t W)$  using text smoothing as reference, and compensate for other modalities via low-rank corrections. Consider vision inputs: ideally we compute  $X_v S_v^{-1} \cdot (S_v W)$ , but using the shared weight produces a residual:

$$\Delta Y = X_v S_v^{-1} \cdot \underbrace{(S_v W - Q(S_t W))}_{\Delta W}. \quad (22)$$

A natural approach is low-rank approximation of  $\Delta W$ . However, directly applying SVD fails: it does not minimize the output residual  $\Delta Y$ , and  $\Delta W$  lacks low-rank structure. Our key insight is that whitening the activations induces low-rank structure. We compute the whitening transform via:

$$\text{SVD}((X_v S_v^{-1})^\top (X_v S_v^{-1})) = P \Lambda P^\top, \quad T = (P \Lambda^{1/2})^\top. \quad (23)$$

which ensures  $(X_v S_v^{-1}) T^{-1}$  is orthonormal. The whitened residual  $T(\Delta W)$  exhibits strong low-rank structure (see Figure 5), enabling accurate approximation via truncated SVD:

$$\text{SVD}(T(\Delta W)) = U \Sigma V^\top \approx U_r \Sigma_r V_r^\top. \quad (24)$$

Inverting the whitening yields the low-rank correction:

$$\Delta W \approx L_1 L_2, \quad \text{where } L_1 = T^{-1} U_r, \quad L_2 = \Sigma_r V_r^\top. \quad (25)$$

**Theorem 2** (Optimal Low-rank Compensation). The rank- $r$  matrix  $L^* = L_1 L_2$ , where  $L_1, L_2$  are given by the rank- $r$  truncated SVD defined in Eq 25, minimizes the reconstruction loss  $\mathcal{L}(L) = \|X_v S_v^{-1}(\Delta W - L)\|_F^2$ , i.e.,

$$L^* = \arg \min_{\text{rank}(L) \leq r} \|X_v S_v^{-1}(\Delta W - L)\|_F^2. \quad (26)$$

*Proof.* Considering only two modalities, text and vision, and performing weight-only quantization exclusively, As defined, we have

$$L^* = T^{-1} (\text{Trunc}_r(T \Delta W)), \quad (27)$$

where  $\text{Trunc}_r(\cdot)$  denotes the best rank- $r$  approximation obtained via truncated SVD., and the whitening matrix  $T = (P \Lambda^{1/2})^\top$ . On the other hand, the SVD decomposition of the covariance matrix is  $(X_v S_v^{-1})^\top (X_v S_v^{-1}) = P \Lambda P^\top$ . It leads to  $X_v S_v^{-1} = U \Lambda^{1/2} P^\top = U T$ , where  $U$  is orthonormal. Therefore, we have

$$\begin{aligned} \mathcal{L}(L^*) &= \|X_v S_v^{-1}(\Delta W - L^*)\|_F^2 \\ &= \|U T(\Delta W - L^*)\|_F^2 \\ &= \|U T(\Delta W - T^{-1} \text{Trunc}_r(T \Delta W))\|_F^2 \\ &= \|T \Delta W - \text{Trunc}_r(T \Delta W)\|_F^2 \\ &= \|\text{SVD}(T \Delta W)\|_F^2 \\ &= \|\text{SVD}(U^{-1} X_v S_v^{-1} \Delta W)\|_F^2 \\ &= \|\text{SVD}(X_v S_v^{-1} \Delta W)\|_F^2 = L_{min}^2. \end{aligned} \quad (28)$$

So the designed SVD truncation ensures the theoretical minimum truncation loss.  $\square$

The theorem 2 shows that SVD-based whitening enables low-rank compensation to effectively bridge modality gaps. The final inference combines the base quantized output with modality-specific corrections:

$$Y = \begin{cases} Q(X_m S_m^{-1}) \cdot Q(S_t W), & m = \text{text} \\ Q(X_m S_m^{-1}) \cdot Q(S_t W) \\ \quad + X_m S_m^{-1} \cdot L_1^m L_2^m. & m \neq \text{text} \end{cases} \quad (29)$$

This maintains a single quantized weight for efficiency while using lightweight low-rank matrices to preserve accuracy across modalities. The complete pipeline is illustrated in Figure 3.

Table 1. Comparison of MASQuant with existing quantization methods on multimodal benchmarks. OCR: OCRBench. Viz: Vizwiz. S-QA: ScienceQA. T-VQA: TextVQA. SQ: SmoothQuant. The best results are highlighted in **bold**.

Method	Bits	Qwen2.5-VL-3B						Qwen2.5-VL-7B					
		MMMU	OCR	Viz	S-QA	T-VQA	Avg	MMMU	OCR	Viz	S-QA	T-VQA	Avg
		Acc↑	Acc↑	Acc↑	Acc↑	Acc↑	Acc↑	Acc↑	Acc↑	Acc↑	Acc↑	Acc↑	Acc↑
Dense	FP16	42.2	79.3	69.1	81.9	77.9	70.1	46.7	83.8	70.8	88.4	82.9	74.5
RTN	W4A16	40.9	77.9	63.0	81.3	75.8	67.8	43.3	83.7	67.8	81.3	82.1	71.6
AWQ		41.9	78.6	<b>68.1</b>	81.7	77.2	69.5	43.3	83.7	70.6	87.8	82.2	73.5
MBQ		41.9	78.5	68.0	81.5	76.8	69.3	44.4	82.8	70.6	87.8	<b>82.9</b>	73.7
MASQuant(ours)		<b>43.3</b>	<b>78.6</b>	67.7	<b>82.4</b>	<b>77.3</b>	<b>69.9</b>	<b>44.4</b>	<b>84.6</b>	<b>71.5</b>	<b>87.8</b>	82.5	<b>74.2</b>
RTN	W8A8	42.6	78.7	68.2	82.4	77.3	69.8	45.6	83.8	70.5	88.1	82.5	74.1
SQ		42.6	79.0	68.0	82.2	77.5	69.9	43.3	83.8	70.0	88.2	82.6	73.6
MBQ		43.3	78.9	<b>68.6</b>	81.8	77.8	70.1	<b>46.7</b>	83.5	70.6	88.5	<b>82.9</b>	74.4
MASQuant(ours)		<b>46.6</b>	<b>79.5</b>	68.2	<b>82.4</b>	<b>77.7</b>	<b>70.9</b>	46.2	<b>84.2</b>	<b>70.6</b>	<b>88.6</b>	82.6	<b>74.4</b>
RTN	W4A8	25.6	0.0	0.0	0.0	0.0	5.1	43.3	68.3	63.2	85.2	76.9	67.4
SQ		25.6	66.9	57.5	72.1	63.9	57.4	37.8	70.2	61.5	83.3	71.1	64.8
MBQ		41.2	66.9	<b>65.0</b>	76.7	<b>73.4</b>	64.6	43.3	<b>74.1</b>	64.3	<b>86.0</b>	74.8	68.5
MASQuant(ours)		<b>46.7</b>	<b>67.2</b>	62.7	<b>77.9</b>	69.2	<b>64.7</b>	<b>43.3</b>	72.8	<b>66.4</b>	85.7	<b>77.0</b>	<b>69.0</b>
SQ	W4A6	22.5	66.7	52.9	69.9	55.9	53.6	28.9	67.7	60.5	78.6	69.3	61.0
MBQ		38.7	65.6	<b>60.5</b>	64.7	<b>69.1</b>	59.7	<b>30.0</b>	<b>71.7</b>	59.8	<b>80.1</b>	72.9	62.9
MASQuant(ours)		<b>40.0</b>	<b>66.7</b>	56.2	<b>71.2</b>	65.3	<b>59.9</b>	29.7	70.3	<b>62.6</b>	79.7	<b>72.9</b>	<b>63.0</b>

Table 2. Comparison of MASQuant with existing quantization methods on omni-modal MLLMs (vision, audio and text). SQ: SmoothQuant. Libri: Librispeech. Wen: Wenetspeech. The best results are highlighted in **bold**.

Method	Bits	Qwen2.5-Omni-3B				Qwen2.5-Omni-7B			
		Audio-Text		Vision-Text	Vision-Audio-Text	Audio-Text		Vision-Text	Vision-Audio-Text
		Libri	Wen	MMMU	Omnibench	Libri	Wen	MMMU	Omnibench
		WER↓	WER↓	Acc↑	Acc↑	WER↓	WER↓	Acc↑	Acc↑
Dense	FP16	3.9	7.5	43.3	43.8	2.9	7.1	50.0	45.3
RTN	W4A16	4.4	9.2	32.2	39.6	3.4	6.7	44.4	43.8
AWQ		9.4	8.0	36.7	43.8	8.7	7.1	47.8	45.3
MBQ		8.2	<b>7.0</b>	38.9	42.6	3.5	6.6	47.8	44.4
MASQuant(ours)		<b>4.0</b>	8.0	<b>39.6</b>	<b>46.9</b>	<b>2.7</b>	<b>7.4</b>	<b>48.8</b>	<b>45.3</b>
RTN	W8A8	3.8	7.6	41.3	37.7	8.2	7.0	48.9	38.4
SQ		<b>3.6</b>	<b>7.5</b>	41.7	44.5	8.2	7.3	48.8	47.6
MBQ		8.9	7.8	41.8	46.1	8.1	7.1	<b>50.0</b>	46.4
MASQuant(ours)		3.8	7.9	<b>42.3</b>	<b>46.1</b>	<b>2.8</b>	<b>6.9</b>	49.9	<b>46.9</b>
RTN	W4A8	109.7	105.6	28.9	29.7	9.0	8.7	42.2	35.2
SQ		77.4	94.2	30.0	27.3	8.6	8.3	42.2	36.7
MBQ		9.5	<b>8.5</b>	27.8	36.7	3.8	8.2	47.8	40.6
MASQuant(ours)		<b>3.6</b>	8.7	<b>36.7</b>	<b>41.4</b>	<b>2.9</b>	<b>8.0</b>	<b>48.8</b>	<b>43.8</b>
RTN	W4A6	87.8	99.6	28.9	23.4	11.8	15.7	28.9	40.6
SQ		87.8	99.5	28.9	18.8	5.8	19.8	<b>37.8</b>	35.9
MBQ		10.8	10.4	31.4	<b>46.9</b>	6.4	14.8	33.3	42.1
MASQuant(ours)		<b>3.7</b>	<b>8.9</b>	<b>32.2</b>	42.2	<b>4.7</b>	<b>8.7</b>	36.8	<b>42.2</b>

## 5. Experiments

### 5.1. Experimental Setups

We evaluate on Qwen2.5-VL [3] and Qwen2.5-Omni [39], multimodal LLMs supporting text, audio, and vision. The architecture of Omni MLLMs includes 675M Vision Transformer-based [8] vision encoder, Whisperlarge-

v3 [26] based audio encoder, LLM Transformer decoder Thinker, speech output Talker, and Streaming Codec Decoder. For generality, we quantize only the LLM component Thinker. We evaluate several state-of-the-art channel-wise smoothing-based quantization methods: AWQ [19], SmoothQuant [37], and MBQ [16]. We evaluate model performance across multiple multimodal benchmarks: Audio-

to-Text Tasks: Evaluated on Librispeech [25] dataset test-other split and Wenetspeech [43] dataset test-net split, using Word Error Rate (WER) as metric. Visual Reasoning Tasks: Evaluated on OCRBench [20], TextVQA [30], Vizwiz [12], ScienceQA [23] and MMMU [42]. Multimodal Reasoning Tasks: Evaluated on OmniBench [17], covering joint text-audio-visual reasoning.

## 5.2. Vision-Language MLLMs

Table 1 evaluates MASQuant on Qwen2.5-VL models. MASQuant matches FP16 performance on both model sizes at W8A8, suggesting that MLLMs can be quantized to 8 bits without accuracy loss when modality-specific characteristics are properly handled. RTN completely fails on W4A8, while SmoothQuant severely degrades. This failure pattern reveals that modality dominance becomes catastrophic at aggressive quantization levels, where smoothing factors dictated by the dominant modality harm the weaker modality.

## 5.3. Vision-Audio-Language MLLMs

Table 2 evaluates quantization on omni-modal models handling vision, audio, and text. The results reveal that modality dominance intensifies as modality diversity increases. At W4A8, SmoothQuant’s audio performance collapses catastrophically on 3B: Librispeech WER jumps from 3.9 to 77.4, and Wenetspeech from 7.5 to 94.2. This 20× degradation, far worse than vision-language failures, demonstrates that audio is completely suppressed when competing with vision and text for smoothing resources. MASQuant maintains near-FP16 audio quality, confirming that per-modality smoothing prevents this collapse. Audio’s vulnerability is intuitive: its smaller activation magnitudes make it the first victim of vision-dominated smoothing factors.

## 5.4. Analysis

**Modality Dominance.** We investigate modality dominance by applying SmoothQuant to Qwen2.5-VL and Qwen2.5-Omni. Figure 4 shows that visual tokens exhibit significantly larger activations than text in both attention and MLP layers. Consequently, smoothing factors track visual distributions while mismatching text by orders of magnitude. This confirms modality dominance is pervasive in MLLMs. We further analyze  $\alpha_i$  distribution, which determines MAS’s SQNR gain. Figures 4c and 4d show non-uniform  $\alpha_i$  across components in both models, validating consistent improvements from MAS.

**Effective Rank.** CMC relies on weight differences having low-rank structure after whitening. We verify this on Qwen2.5-VL/Omni-3B using effective rank (lower is better). As shown in Figure 5, whitening reduces effective rank substantially, confirming our design.

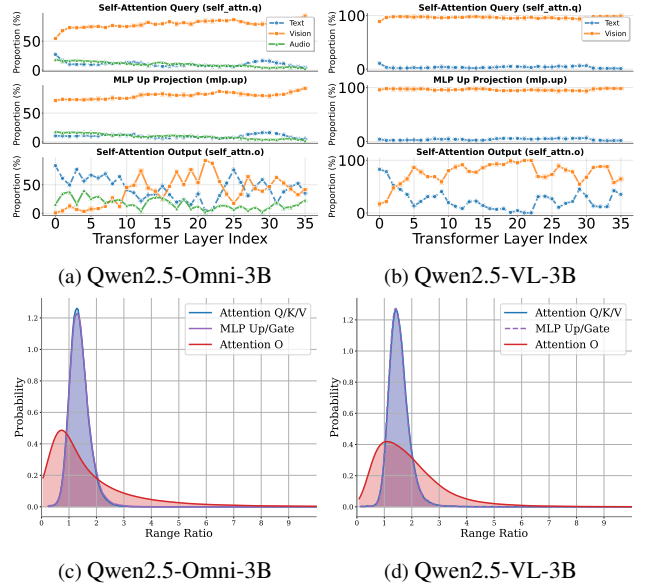


Figure 4. Percentage of unified smoothing factors from different modalities using SmoothQuant on Omni and VL MLLMs.

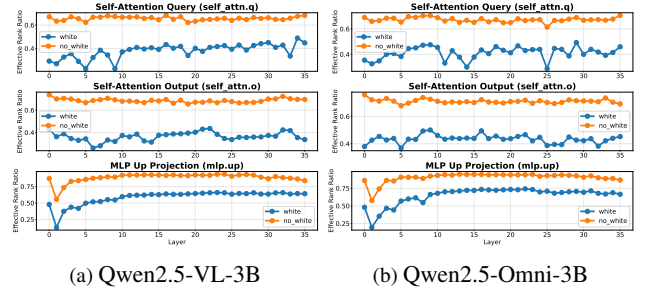


Figure 5. Effective ranks of  $\Delta W$  is reduced across layers after SVD-based Whitening b SQNR improves as the rank ratio increases on both Qwen2.5-VL-3B and Qwen2.5-Omni-3B.

**The Effect of MAS.** Table 3 reveals the necessity of modality-aware smoothing in W4A8 quantization. The most striking result is on LibriSpeech: uniform smoothing yields 77.4 WER while MAS achieves 3.8 WER. This dramatic gap exposes a fundamental failure mode where uniform smoothing catastrophically degrades the weaker modality when forced to compromise between modalities with disparate activation ranges. Notably, learnable optimization amplifies rather than closes this gap.

**Modality Loss Weight.** Table 4 shows ablation results of  $\lambda_t$  and  $\lambda_v$  on Qwen2.5-VL-3B. Equal smoothing works best: 17.2 PPL and 56.9% average accuracy. Reducing vision smoothing to  $\lambda_v=0.5$  drops MMMU from 37.8 to 30.0 with minimal text benefit. Further reducing to 0.1 collapses PPL to 33.7. Reducing text smoothing ( $\lambda_t=0.5$ ) degrades all metrics. In this work, we set  $\lambda_t=\lambda_v=1.0$ .

Table 3. Effects of Modality-Aware Smoothing (W4A8).

Method	Opt.	Omni-3B		VL-3B	
		Libri	OmniB.	T-VQA.	MMMU
Uniform		77.4	27.3	51.3	25.6
MAS		<b>3.8</b>	<b>36.7</b>	<b>54.7</b>	<b>28.9</b>
Uniform	✓	6.0	33.3	65.0	33.3
MAS	✓	<b>3.6</b>	<b>47.7</b>	<b>68.2</b>	<b>46.7</b>

Table 4. Effects of Modality Loss Weight (W4A8).

$\lambda_t$	$\lambda_v$	Qwen2.5-VL-3B				
		PPL	MMMU	T-VQA.	S-QA	Avg
1.0	1.0	17.2	37.8	55.2	77.8	56.9
1.0	0.5	17.8	30.0	57.8	80.0	55.9
1.0	0.1	33.7	32.2	65.4	76.7	58.1
0.5	1.0	17.3	33.3	53.9	68.9	52.0

**Training Epochs.** Table 5 shows convergence on Qwen2.5-VL-3B. Performance improves rapidly: PPL drops from 23.9 to 17.0. Average accuracy peaks at epoch 2, then slightly declines. We use 2 epochs—a good trade-off between efficiency and performance.

Table 5. Effects of Modality-Aware Smoothing (W4A8).

Epoch	Qwen2.5-VL-3B				
	PPL	MMLU	T-VQA.	S-QA	Avg
1	23.9	38.9	52.2	79.5	56.9
2	18.6	37.8	67.5	78.4	61.2
5	17.6	34.4	65.9	77.4	59.2
10	17.0	37.8	68.2	76.5	60.8

**The Effect of CMC.** Figure 6 plots SQNR vs. rank ratio. CMC dominates the Non-Whitened baseline in the low-rank regime, reducing the rank required to match MBQ by 4x. Specifically, CMC surpasses MAS at ratio of 0.08 and saturates near 3.5 SQNR, whereas the baseline struggles to match MBQ until a ratio of 0.4.

Table 6. Computation cost and memory at decoding phase, where  $d$  is hidden size,  $r$  is rank, and  $m$  is the number of extra modalities.

Base modality	Computation	Memory
Text	$d$	0
Others	$d + 2rd$	$2mrd$

**Base Modality Choice.** We choose text as the base modality to decouple CMC from decoding. As shown in Table 6, other modalities would require CMC involvement, leading to extra costs of computation and memory.

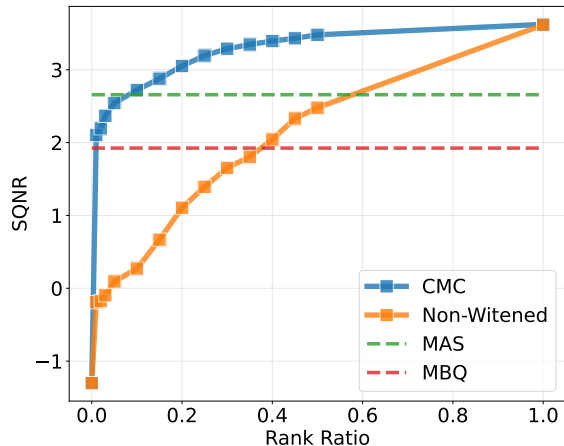


Figure 6. SQNR as a function of rank ratio for CMC on Qwen2.5-Omni-3B under W4A6 quantization. MAS applies independent modality-specific smoothing. MBQ employs a uniform factor optimized by modality balance reconstruction.

## 5.5. Inference Speed Up

To validate practical efficiency, we implement a custom CUDA kernel based on Nunchaku [15] that fuses projection and quantization operators to minimize memory access. A multi-modal mask efficiently manages conditional low-rank execution. Table 7 shows that MASQuant achieves a 2.5x speedup over FP16 with marginal latency overhead (5–10%) compared to MBQ, while maintaining identical decoding latency.

Table 7. End-to-end prefill-stage performance of Qwen2.5-VL-7B on Desktop RTX 4090 with fused GPU kernels (sequence length = 2048) under W4A4 setting. MAS: MASQuant. BS: Batch Size.

BS	Method	Rank Ratio	Prefill (ms)	Speedup	Mem (GB)	Mem Saving
1	FP16	-	191.82	/	13.73	/
	MBQ	-	68.65	<b>2.79</b> ×	4.85	<b>2.83</b> ×
	MAS	0.01	71.62	<b>2.67</b> ×	4.97	<b>2.76</b> ×
	MAS	0.02	72.89	<b>2.63</b> ×	5.04	<b>2.73</b> ×
	MAS	0.05	77.10	<b>2.49</b> ×	5.37	<b>2.56</b> ×
8	FP16	-	2146.01	/	17.27	/
	MBQ	-	643.68	<b>3.33</b> ×	8.89	<b>1.94</b> ×
	MAS	0.01	649.29	<b>3.30</b> ×	9.02	<b>1.92</b> ×
	MAS	0.02	657.68	<b>3.26</b> ×	9.08	<b>1.90</b> ×
	MAS	0.05	696.44	<b>3.07</b> ×	9.42	<b>1.83</b> ×

## 6. Conclusion

In this work, we identify smoothing misalignment as the primary obstacle preventing channel-wise smoothing from applying to MLLMs. To address this, we propose the MASQuant which applies Modality-aware Smoothing and Cross-Modal Compensation to support modality-specific smoothing factors and single quantized weight during inference. Our approach is simple and highly effective. We demonstrate its efficacy on multi-modal benchmark.

## References

- [1] Josh Achiam, Steven Adler, Sandhini Agarwal, Lama Ahmad, Ilge Akkaya, Florencia Leoni Aleman, Diogo Almeida, Janko Altenschmidt, Sam Altman, Shyamal Anadkat, et al. Gpt-4 technical report. *arXiv preprint arXiv:2303.08774*, 2023. 1
- [2] Saleh Ashkboos, Amirkeivan Mohtashami, Maximilian L Croci, Bo Li, Pashmina Cameron, Martin Jaggi, Dan Alistarh, Torsten Hoefler, and James Hensman. Quarot: Outlier-free 4-bit inference in rotated llms. *Advances in Neural Information Processing Systems*, 37:100213–100240, 2024. 2
- [3] Shuai Bai, Keqin Chen, Xuejing Liu, Jialin Wang, Wenbin Ge, Sibao Song, Kai Dang, Peng Wang, Shijie Wang, Jun Tang, et al. Qwen2. 5-vl technical report. *arXiv preprint arXiv:2502.13923*, 2025. 1, 6
- [4] Yelysei Bondarenko, Riccardo Del Chiaro, and Markus Nagel. Low-rank quantization-aware training for llms. *arXiv preprint arXiv:2406.06385*, 2024. 2
- [5] Jerry Chee, Yaohui Cai, Volodymyr Kuleshov, and Christopher M De Sa. Quip: 2-bit quantization of large language models with guarantees. *Advances in Neural Information Processing Systems*, 36:4396–4429, 2023. 2
- [6] Mengzhao Chen, Wenqi Shao, Peng Xu, Jiahao Wang, Peng Gao, Kaipeng Zhang, and Ping Luo. Efficientqat: Efficient quantization-aware training for large language models. *arXiv preprint arXiv:2407.11062*, 2024. 2
- [7] Tim Dettmers, Ruslan Svirschevski, Vage Egiazarian, Denis Kuznedelev, Elias Frantar, Saleh Ashkboos, Alexander Borzunov, Torsten Hoefler, and Dan Alistarh. Spqr: A sparse-quantized representation for near-lossless llm weight compression. *arXiv preprint arXiv:2306.03078*, 2023. 2
- [8] Alexey Dosovitskiy, Lucas Beyer, Alexander Kolesnikov, Dirk Weissenborn, Xiaohua Zhai, Thomas Unterthiner, Mostafa Dehghani, Matthias Minderer, Georg Heigold, Sylvain Gelly, et al. An image is worth 16x16 words: Transformers for image recognition at scale. *arXiv preprint arXiv:2010.11929*, 2020. 6
- [9] Abhimanyu Dubey, Abhinav Jauhri, Abhinav Pandey, Abhishek Kadian, Ahmad Al-Dahle, Aiesha Letman, Akhil Mathur, Alan Schelten, Amy Yang, Angela Fan, et al. The llama 3 herd of models. *arXiv e-prints*, pages arXiv–2407, 2024. 1
- [10] Elias Frantar, Saleh Ashkboos, Torsten Hoefler, and Dan Alistarh. Gptq: Accurate post-training quantization for generative pre-trained transformers. *arXiv preprint arXiv:2210.17323*, 2022. 2
- [11] Chaoyou Fu, Yuhan Dai, Yongdong Luo, Lei Li, Shuhuai Ren, Renrui Zhang, Zihan Wang, Chenyu Zhou, Yunhang Shen, Mengdan Zhang, et al. Video-mme: The first-ever comprehensive evaluation benchmark of multi-modal llms in video analysis. In *Proceedings of the Computer Vision and Pattern Recognition Conference*, pages 24108–24118, 2025. 1
- [12] Danna Gurari, Qing Li, Abigale J Stangl, Anhong Guo, Chi Lin, Kristen Grauman, Jiebo Luo, and Jeffrey P Bigham. Vizwiz grand challenge: Answering visual questions from blind people. In *Proceedings of the IEEE conference on computer vision and pattern recognition*, pages 3608–3617, 2018. 7
- [13] Jacob Kahn, Morgane Riviere, Weiyi Zheng, Evgeny Kharitonov, Qiantong Xu, Pierre-Emmanuel Mazaré, Julien Karadayi, Vitaliy Liptchinsky, Ronan Collobert, Christian Fuegen, et al. Libri-light: A benchmark for asr with limited or no supervision. In *ICASSP 2020-2020 IEEE International Conference on Acoustics, Speech and Signal Processing (ICASSP)*, pages 7669–7673. IEEE, 2020. 1
- [14] Sehoon Kim, Coleman Hooper, Amir Gholami, Zhen Dong, Xiuyu Li, Sheng Shen, Michael W Mahoney, and Kurt Keutzer. Squeezellm: Dense-and-sparse quantization. *arXiv preprint arXiv:2306.07629*, 2023. 2
- [15] Muyang Li, Yujun Lin, Zhekai Zhang, Tianle Cai, Xiuyu Li, Junxian Guo, Enze Xie, Chenlin Meng, Jun-Yan Zhu, and Song Han. Svdquant: Absorbing outliers by low-rank components for 4-bit diffusion models. *arXiv preprint arXiv:2411.05007*, 2024. 8
- [16] Shiyao Li, Yingchun Hu, Xuefei Ning, Xihui Liu, Ke Hong, Xiaotao Jia, Xiuhong Li, Yaqi Yan, Pei Ran, Guohao Dai, et al. Mbg: Modality-balanced quantization for large vision-language models. In *Proceedings of the Computer Vision and Pattern Recognition Conference*, pages 4167–4177, 2025. 1, 2, 3, 4, 6
- [17] Yizhi Li, Ge Zhang, Yinghao Ma, Ruibin Yuan, Kang Zhu, Hangyu Guo, Yiming Liang, Jiaheng Liu, Zekun Wang, Jian Yang, et al. Omnibench: Towards the future of universal omni-language models. *arXiv preprint arXiv:2409.15272*, 2024. 1, 7
- [18] Haokun Lin, Haobo Xu, Yichen Wu, Jingzhi Cui, Yingtao Zhang, Linzhan Mou, Linqi Song, Zhenan Sun, and Ying Wei. Duquant: Distributing outliers via dual transformation makes stronger quantized llms. *Advances in Neural Information Processing Systems*, 37:87766–87800, 2024. 2
- [19] Ji Lin, Jiaming Tang, Haotian Tang, Shang Yang, Wei-Ming Chen, Wei-Chen Wang, Guangxuan Xiao, Xingyu Dang, Chuang Gan, and Song Han. Awq: Activation-aware weight quantization for on-device llm compression and acceleration. *Proceedings of machine learning and systems*, 6:87–100, 2024. 1, 2, 3, 6
- [20] Yuliang Liu, Zhang Li, Mingxin Huang, Biao Yang, Wenwen Yu, Chunyuan Li, Xu-Cheng Yin, Cheng-Lin Liu, Lianwen Jin, and Xiang Bai. Ocrbench: on the hidden mystery of ocr in large multimodal models. *Science China Information Sciences*, 67(12):220102, 2024. 7
- [21] Zechun Liu, Barlas Oguz, Changsheng Zhao, Ernie Chang, Pierre Stock, Yashar Mehdad, Yangyang Shi, Raghuraman Krishnamoorthi, and Vikas Chandra. Llm-qat: Data-free quantization aware training for large language models. *arXiv preprint arXiv:2305.17888*, 2023. 2
- [22] Zechun Liu, Changsheng Zhao, Igor Fedorov, Bilge Soran, Dhruv Choudhary, Raghuraman Krishnamoorthi, Vikas Chandra, Yuandong Tian, and Tijmen Blankevoort. Spinquant: Llm quantization with learned rotations. *arXiv preprint arXiv:2405.16406*, 2024. 2

- [23] Pan Lu, Swaroop Mishra, Tanglin Xia, Liang Qiu, Kai-Wei Chang, Song-Chun Zhu, Oyvind Tafjord, Peter Clark, and Ashwin Kalyan. Learn to explain: Multimodal reasoning via thought chains for science question answering. *Advances in Neural Information Processing Systems*, 35:2507–2521, 2022. 7
- [24] Yuexiao Ma, Huixia Li, Xiawu Zheng, Feng Ling, Xuefeng Xiao, Rui Wang, Shilei Wen, Fei Chao, and Rongrong Ji. Affinequant: Affine transformation quantization for large language models. *arXiv preprint arXiv:2403.12544*, 2024. 1, 2
- [25] Vassil Panayotov, Guoguo Chen, Daniel Povey, and Sanjeev Khudanpur. Librispeech: an asr corpus based on public domain audio books. In *2015 IEEE international conference on acoustics, speech and signal processing (ICASSP)*, pages 5206–5210. IEEE, 2015. 7
- [26] Alec Radford, Jong Wook Kim, Tao Xu, Greg Brockman, Christine McLeavey, and Ilya Sutskever. Robust speech recognition via large-scale weak supervision. In *International conference on machine learning*, pages 28492–28518. PMLR, 2023. 6
- [27] Wenqi Shao, Mengzhao Chen, Zhaoyang Zhang, Peng Xu, Lirui Zhao, Zhiqian Li, Kaipeng Zhang, Peng Gao, Yu Qiao, and Ping Luo. Omniquant: Omnidirectionally calibrated quantization for large language models. *arXiv preprint arXiv:2308.13137*, 2023. 1, 2, 3
- [28] Tao Sheng, Chen Feng, Shaojie Zhuo, Xiaopeng Zhang, Liang Shen, and Mickey Aleksic. A quantization-friendly separable convolution for mobilenets. In *2018 1st workshop on energy efficient machine learning and cognitive computing for embedded applications (EMC2)*, pages 14–18. IEEE, 2018. 4
- [29] Amanpreet Singh, Vivek Natarajan, Meet Shah, Yu Jiang, Xinlei Chen, Dhruv Batra, Devi Parikh, and Marcus Rohrbach. Towards vqa models that can read. In *Proceedings of the IEEE/CVF conference on computer vision and pattern recognition*, pages 8317–8326, 2019. 1
- [30] Amanpreet Singh, Vivek Natarajan, Meet Shah, Yu Jiang, Xinlei Chen, Dhruv Batra, Devi Parikh, and Marcus Rohrbach. Towards vqa models that can read. In *Proceedings of the IEEE/CVF conference on computer vision and pattern recognition*, pages 8317–8326, 2019. 7
- [31] Yuxuan Sun, Ruikang Liu, Haoli Bai, Han Bao, Kang Zhao, Yuening Li, Jiaxin Hu, Xianzhi Yu, Lu Hou, Chun Yuan, et al. Flatquant: Flatness matters for llm quantization. *arXiv preprint arXiv:2410.09426*, 2024. 1, 2
- [32] Qwen Team. Qwen2 technical report. *arXiv preprint arXiv:2407.10671*, 2024. 1
- [33] Mart Van Baalen, Andrey Kuzmin, Ivan Koryakovskiy, Markus Nagel, Peter Couperus, Cedric Bastoul, Eric Mahurin, Tijmen Blankevoort, and Paul Whatmough. Gptvq: The blessing of dimensionality for llm quantization. *arXiv preprint arXiv:2402.15319*, 2024. 4
- [34] Xin Wang, Yu Zheng, Zhongwei Wan, and Mi Zhang. Svd-llm: Truncation-aware singular value decomposition for large language model compression. *arXiv preprint arXiv:2403.07378*, 2024. 2
- [35] Xin Wang, Samiul Alam, Zhongwei Wan, Hui Shen, and Mi Zhang. Svd-llm v2: Optimizing singular value truncation for large language model compression. *arXiv preprint arXiv:2503.12340*, 2025. 2
- [36] Xiuying Wei, Yunchen Zhang, Xiangguo Zhang, Ruihao Gong, Shanghang Zhang, Qi Zhang, Fengwei Yu, and Xianglong Liu. Outlier suppression: Pushing the limit of low-bit transformer language models. *Advances in Neural Information Processing Systems*, 35:17402–17414, 2022. 1
- [37] Guangxuan Xiao, Ji Lin, Mickael Seznec, Hao Wu, Julien Demouth, and Song Han. Smoothquant: Accurate and efficient post-training quantization for large language models. In *International conference on machine learning*, pages 38087–38099. PMLR, 2023. 1, 2, 3, 6
- [38] Jingjing Xie, Yuxin Zhang, Mingbao Lin, Liujuan Cao, and Rongrong Ji. Advancing multimodal large language models with quantization-aware scale learning for efficient adaptation. In *Proceedings of the 32nd ACM International Conference on Multimedia*, pages 10582–10591, 2024. 2
- [39] Jin Xu, Zhifang Guo, Jinzheng He, Hangrui Hu, Ting He, Shuai Bai, Keqin Chen, Jialin Wang, Yang Fan, Kai Dang, et al. Qwen2. 5-omni technical report. *arXiv preprint arXiv:2503.20215*, 2025. 1, 6
- [40] Zhewei Yao, Xiaoxia Wu, Cheng Li, Stephen Youn, and Yuxiong He. Zeroquant-v2: Exploring post-training quantization in llms from comprehensive study to low rank compensation. *arXiv preprint arXiv:2303.08302*, 2023. 2
- [41] Jiang Yong Yu, Sifan Zhou, Dawei Yang, Shuo Wang, Shuoyu Li, Xing Hu, Chen Xu, Zukang Xu, Changyong Shu, and Zhihang Yuan. Mquant: Unleashing the inference potential of multimodal large language models via full static quantization. *arXiv preprint arXiv:2502.00425*, 2025. 1, 2, 3
- [42] Xiang Yue, Yuansheng Ni, Kai Zhang, Tianyu Zheng, Ruoqi Liu, Ge Zhang, Samuel Stevens, Dongfu Jiang, Weiming Ren, Yuxuan Sun, et al. Mmmu: A massive multi-discipline multimodal understanding and reasoning benchmark for expert agi. In *Proceedings of the IEEE/CVF Conference on Computer Vision and Pattern Recognition*, pages 9556–9567, 2024. 1, 7
- [43] Binbin Zhang, Hang Lv, Pengcheng Guo, Qijie Shao, Chao Yang, Lei Xie, Xin Xu, Hui Bu, Xiaoyu Chen, Chenchen Zeng, et al. Wenetspeech: A 10000+ hours multi-domain mandarin corpus for speech recognition. In *ICASSP 2022-2022 IEEE International Conference on Acoustics, Speech and Signal Processing (ICASSP)*, pages 6182–6186. IEEE, 2022. 1, 7
- [44] Weibo Zhao, Yubin Shi, Xinyu Lyu, Wanchen Sui, Shen Li, and Yong Li. Aser: activation smoothing and error reconstruction for large language model quantization. In *Proceedings of the AAAI Conference on Artificial Intelligence*, pages 22822–22830, 2025. 2
- [45] Zhen Zheng, Xiaonan Song, and Chuanjie Liu. Mixllm: Llm quantization with global mixed-precision between output-features and highly-efficient system design. *arXiv preprint arXiv:2412.14590*, 2024. 2